ORIGINAL SCIENTIFIC PAPER

CROATICA CHEMICA ACTA

Croat. Chem. Acta **2020**, *93*(1), 41–47
Published online: August 22, 2020
DOI: 10.5562/cca3614

HKD 1926

Mn(III) Catalyzed Electrochemical Reduction of CO_2 on Carbon Electrodes

Khalaf M. Alenezi

Department of Chemistry, College of Science, University of Ha'il, 81451, Kingdom of Saudi Arabia
Author's e-mail address: k.alenezi@uoh.edu.sa

RECEIVED: February 2, 2020 ✶ REVISED: August 11, 2020 ✶ ACCEPTED: August 18, 2020

Abstract: Though challenging, conversion of carbon dioxide (CO_2) to valuable products is an emerging area of research. Electrochemical reduction (ECR) has emerged as an efficient and rapid technique to achieve this goal. Herein, 5,10,15,20-tetraphenyl-21H, 23H-porphine manganese(III) chloride [(Mn(TPP)Cl)] catalyzed CO_2 reduction at vitreous carbon electrode in acetonitrile electrolyte is reported. The effect of catalyst concentration, addition of Brönsted acid (CF_3CH_2OH) to CO_2-saturated solution have been studied and reported. Based on the results, possible mechanistic pathways have also been suggested and discussed.

Keywords: acetonitrile, electrochemical reduction (ECR), Mn(TPP)Cl.

INTRODUCTION

FOLLOWING the first industrial revolution, a significant amount of carbon dioxide (CO_2) has already been emitted to the atmosphere leading to global warming, icecaps melting, ocean acidification and other fates.[1,2] This issue, along with rapid increase human population, is a matter of serious concern, especially when the level of non-renewable energies is constantly declining. In the last few decades, a significant amount of research has been carried out to convert CO_2 to industrially useful precursor(s) such as carbon monoxide (CO), formaldehyde (HCHO), methanol (CH_3OH), methane (CH_4) and other hydrocarbons.[3,4] These chemical conversion can be achieved through different techniques and one of them is CO_2 reduction using electrons, i.e. electrochemical reduction (ECR).[5,6] Since CO_2 is thermodynamically stable molecule and requires large potential (overpotential) to break C-O bonds, a homo- or heterogeneous catalyst is often employed during the reduction process. Therefore, obtaining a stable and efficient electrocatalyst highly needed. Owing to this, a large number of organic and organometallic architectures with CO_2 reducing ability has been reported.[6–11] Compared to organic counterpart, organometallic framework serve as a better catalytic platform due to their redox features, tunable coordination and geometry around the metal center. Despite the fact that several group 6–10 metal complexes are available with excellent catalytic activities, selectivity of the reduced products and cost-effectiveness remains a big challenge.[12–14] Considering these, researchers turned towards systems with inexpensive nature and high abundance. In this context, a range of metal complex decorated with functionalized organic ligands have been reported with varying activity. It was noted that when a metal core is embedded within a macrocyclic receptor (such as porphyrin), a synergism in catalysis could be accomplished.[15,16] In the last few decades, several metalloporphyrins for electrocatalytic and photo-electro-catalytic reduction of CO_2 have been reported.[17–20] It has been demonstrated that a minor variation (functionalization) of the ligand core or change in the metal center has a significant effect on overpotential, Faradaic efficiency (FE), turn over frequency (TOF), turnover number (TON) and selectivity of the products.[17] For example, Savéant and co-workers reported an elegant water-soluble Fe(II) porphyrin catalyst with high efficiency and selectivity in neutral aqueous solution (pH = 6.7).[21] The reported catalyst yielded 90 % CO, 7 % H_2 and very small amounts of acetate, formate, and oxalate as electrolyzed product with an applied potential of –0.97 V *vs* SHE. The fact that the catalyst exhibited excellent

ECR performance in aqueous solution, it is particularly useful for industrial applications. Mechanistically, both metal and ligand centered mechanism has been suggested for the ECR. A recent DFT calculation on such systems indicated that redox non-innocent porphyrin ligand accept two electrons and one proton, while the metal ion keeps its oxidation state unchanged during the reduction process.[22]

Similarly, Mn-complexes have emerged as excellent molecular ECR catalysts with superb activity and selectivity. It has been demonstrated that, using a Mn-complex, CO_2 reduction can be performed under mild conditions and at lower overpotential.[23–28] For instance, a combination of Zn-(TPP) (as photosensitizer) and Mn(III) bipyridine (as catalyst) actively reduces CO_2 (TON = 119) with very high selectivity (86 %).[29] Inspired by the intriguing properties of porphyrin core and catalytic activities of Mn(III) complexes, we carried out this study to investigate the performance of a Mn(III) complex for ECR of CO_2. The study was carried out using Mn(TPP)Cl complex (Figure 1) at vitreous carbon electrode in the acetonitrile (MeCN) electrolyte and the results of the findings are discussed herein.

EXPERIMENTAL

Mn(TPP)Cl and Et_3N.HCl were purchased from Aldrich and used as received. Acetonitrile (MeCN) was purified by distillation over calcium hydride. Autolab PGSTAT 128 potentiostat / Galvanise (NOVA 1.10 software) was used for all cyclic voltammetric experiments and the potentiostat connected with three electrodes: carbon working electrode (area = 0.07 cm^2), a platinum gauze (2 cm^2) as an auxiliary electrode, and Ag^+/AgCl as a reference electrode. The electrochemical cells were degassed with argon (Ar) gas to remove oxygen and filled with an electrolyte (a solvent containing 0.1 M $[Bu_4N][BF_4]$). The volume of the working electrode compartment was 14 mL. 0.5 mM Mn(TPP)Cl was dissolved in 5 mL dry DMF and stirred under Ar in electrochemical cell for 10 mins and then the solution was saturated with CO_2. The cyclic voltammetry of Mn(TPP)Cl was carried out in the absence and presence of CO_2. Brönsted acid (CF_3CH_2OH) of different concentration (0.05 M, 0.2 M , 0.4 M and 0.6 M) was added to improve both the efficiency and catalyst lifetime. In the end, the electrolysis was carried out at -1.3 V/ Ag^+lAgCl and the current and the charges passed were recorded during the course of electrolysis *vs* the time. The electrolysis was stopped when the current decayed after 3 h. Bulk electrolysis experiments were carried out in a three compartment H-type cell. A carbon electrode (cathode, area 2 cm^2) was employed for conventional electrolyses. Turn over number (TON) was calculated as the *n*(CO) / *n*(catalyst). Reaction products were analyzed using a Perkin–Elmer Clarius 500 gas chromatography fitted with a 5Å molecular sieve column (800/100 mesh, 6' × 1/8") and thermal conductivity detector (GC-TCD). The operating conditions were as follows: 80 °C oven temperature, 0.5 mL injection volume, and 10 min retention time. The external standard calibration was performed following the previously reported protocol.[30]

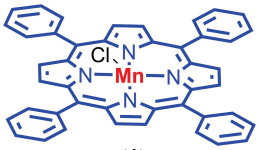

(**1**)

Figure 1. Chemical structure of 5,10,15,20-Tetraphenyl-21H,23H-porphine manganese(III) chloride [(Mn(TPP)Cl)].

RESULTS AND DISCUSSION

Electrochemical Behavior of Mn(TPP)Cl

The cyclic voltammogram (CV) of Mn(TPP)Cl recorded in 0.1 M $[Bu_4N][BF_4]$-MeCN under Ar (Figure 2) displayed two redox pairs (–0.15 V and –1.3 V *vs* Ag/AgCl). In a recent work, Marianov and Jiang[31] reported that Mn(TPP) display two reduction peaks at −0.70 and −1.81 V (*vs* Fc^+/Fc in TBAP-DMF electrolyte), corresponding to Mn(III)/Mn(II) and Mn(II)/Mn(I) couples. On the contrary, they found that a free-base tetraphenyl porphyrin ligand exhibit weak redox response centered around –1.60 V. Based on these information, the first $1e^-$ reduction of Mn(TPP)Cl can be ascribed to Mn(III)/Mn(II) while the second reduction to Mn(II)/Mn(I).

Under the same condition, the plot of i_p^{red} versus $\nu^{1/2}$ of Mn^{2+} /Mn^{1+} process was reported, which is diffusion controlled, involves an electrochemically reversible one-electron transfer. The plots of second reduction wave $^{I}i_p^{red}$ versus $\nu^{1/2}$ show that the plot is linear which prove that there is no complicated mass transfer control of one electron-transfer rate.[32]

CV of Mn(TPP)Cl Under CO_2 and the Effect of CF_3CH_2OH

The CV of Mn(TPP)Cl (0.5 mM) as electrocatalysts in MeCN at vitreous carbon is given in Figure 2. From the CV, it is clear that CO_2 interacted with the reduced catalyst [Mn(I)] at the second reduction wave (–1.3 V vs Ag/AgCl) of Mn(TPP)Cl as evident from an increase in peak current ($^{III}i_p$). Indeed, this value was found to be lower than other related systems such as Co(TPP)Cl (at –1.85 V) , and Fe(TPP)Cl (at –1.65 V).[33,34] The peak current was 1.3×10^{-5} A in the absence of CO_2 which raised to 2.1×10^{-5} A upon the addition of CO_2. Besides, potential also shifted towards

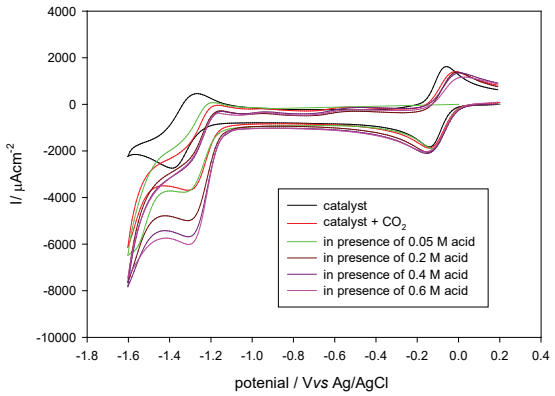

Figure 2. Cyclic voltammetry of 0.5 mM Mn(TPP)Cl under Ar, under CO_2 (at 1 atmosphere) in the presence of different concentration of CF_3CH_2OH. Scan rate 100 mV s^{-1}, vitreous carbon electrode at 25 °C.

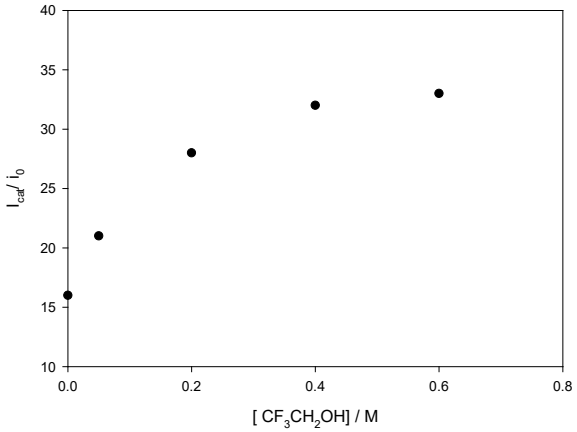

Figure 3. The effect of acid concentration on i_{cat}/i_0 ratio at a vitreous carbon electrode. i_{cat} is the peak catalytic current calculated at 100 mV s^{-1} and i_o is the peak current measured for the one-electron reduction step.

positive (about 30 mV) in the presence of CO_2. However, a small increase in the value of peak current was indicative of slow electrocatalysis (~ two times).

In the past, Saveant and co-workers[35,36] demonstrated that the addition of a proton source often improves the current efficiency of CO_2 reduction and increase the catalyst stability. The CO_2 reduction in acidic media occurs as per the following equation [Eq. (1)]:

$$CO_2 + 2H^+ + 2e^- \longrightarrow CO + H_2O \quad (1)$$

To underpin the effect of acid addition on Mn(TPP)Cl catalyzed ECR of CO_2, Brönsted acid (CF_3CH_2OH) was added and the changes were monitored. Figure 2 shows the variation of peak current as a function [CF_3CH_2OH]. It is clear from the figure that the addition of CF_3CH_2OH led to a dramatic increase in the value of catalytic current, possibly due to the stabilization of metal-CO_2 adduct. Notably, the current density increases up to ~ 0.4 M of CF_3CH_2OH, after which the electrocatalysis becomes independent of the acid concentration, indicating protonation is no longer rate limiting. Also, the addition of excess CF_3CH_2OH led to the precipitation of Mn(TPP)Cl.

Calculation of k_{cat} at Carbon Electrode

Basically, k_{cat} is measured to know at what concentration i_{cat}/i_o ratio (i_{cat} is the peak catalytic current calculated at 100 mV s^{-1} and i_o is the peak current measured for the one-electron reduction step) becomes independent of the acid concentration. It is determined as per the following equation [Eq. (2)]:

$$k_{cat} = k_{obs} / [CO_2] \quad (2)$$

where the concentration of CO_2 in MeCN was 0.25 M at 23 °C. Figure 3 shows the plot between i_{cat}/i_o ratio *vs* varying concentration of CF_3CH_2OH under CO_2 and in the presence of 0.5 mM Mn(TPP)Cl. According to the data obtained, it was noted that the i_{cat}/i_o become independent of the acid concentration at ~ 0. 4 M.

Using the above data, the value of the rate constant (k_{obs}) at vitreous carbon electrode can be calculated as [Eq. (3)]:[8,37]

$$k_{obs} = 0.1992\ (n^2\ F\ v\ /\ (R\ T)\ (i_{cat}\ /\ i_0)^2 \quad (3)$$

where n is the number of electrons involved in the turnover, F is Faraday constant, v is scan rate, R is the gas constant, and T is temperature. In the acid independent regime, the rate constant (k_{cat}, 23 °C) for the catalysis at vitreous carbon was estimated to be 0.12×10^2 M^{-1} s^{-1}, considering the saturated concentration of CO_2 in MeCN to be 0.25 M at 23 °C.

Preparative Scale Electrocatalysis

Preparative scale electrocatalysis was carried out at –1.4 V in 0.1 M [Bu_4N][BF_4]-MeCN solution for 3 h at room temperature. The amount of catalyst was 0.5 mM while acid (CF_3CH_2OH) was 0.6 M. Charge (Q) was calculated using the equation [Eq. (4)]:

$$Q = n\ N\ F \quad (4)$$

where Q is the charge (coulombs) passed, n is the number of electrons involved, N represents the amount of complex (in moles), and F is the Faraday constant (96485 C mol^{-1}). Under

the above-said conditions, it was noted that the catalyst selectively reduced CO_2 to CO (54 %, 14.8 µmole) with the turnover number (TON) = 6 and charged passed = 5.3 C (Table 1). Besides, H_2 was also generated as the second major product (38 %, 10.3 µmole) along with some unidentified products (~ 8 %); possibly carbonate or formic acid (see the mechanism, *vide-infra*).[38] Besides, when electrocatalysis was carried out in absence of CF_3CH_2OH under similar conditions, very small amount of CO was observed (8 %), indicating the crucial role of acid in the catalytic process.

The yield of the ECR varies proportionally with the electrolysis time (Table 2). For example, after 0.5 h, the current efficiency was 32 %, leading to the generation of 2.0 µmol of CO. On the other hand, after 3 h of electrocatalysis, the current efficiency was 52 % with 11.8 µmol of CO. Figure 4 shows the decay of current with time at potential –1.4 V (Ag/AgCl). As can be seen, the electrolysis stopped when the current decay to 20 % of initial current. Moreover, the rate of decay was lower in the presence of acid as compared to decay in the absence of acid.

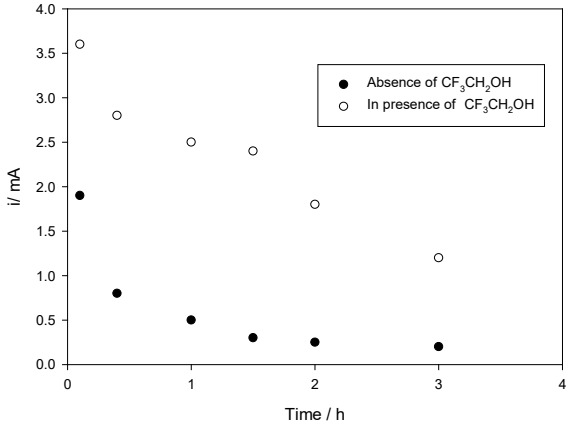

Figure 4. Decay of current with electrolysis time both in presence and absence of CF_3CH_2OH. (● indicates "in presence of acid" and ○ indicates "in absence of acid").

Table 2. Data for ECR of CO_2 by (0.5 mM, 2.5 µmol) Mn(TPP)Cl at carbon electrode.

Time/h	0.5	1	1.5	2	2.5	3
n(CO) / µmol	2.07	4.9	8.45	10.3	11.1	11.8
Current efficiency / %	32	41	45	50	51	52
T.N	0.8	1.98	3.4	4.1	4.4	4.7
Charge passed, C	1.3	2.3	3.6	3.9	4.2	4.3

Table 1. Current efficiencies of ECR of CO_2 in the presence and absence of Mn(TPP)Cl.

	CPE Potential (Ag/AgCl / V)	amount of catalyst / µmol	Time / h	Charge / C	Current efficiency of CO	Current efficiency of H_2
In the presence of Mn(TPP)Cl and CF_3CH_2OH	–1.4	0.5	3	5.3	54	38
In the presence of Mn(TPP)Cl without F_3CH_2OH	–1.4	0.5	3	1.4	8	-
Control experiment	–1.4	0	3	2.1	Negligible	75

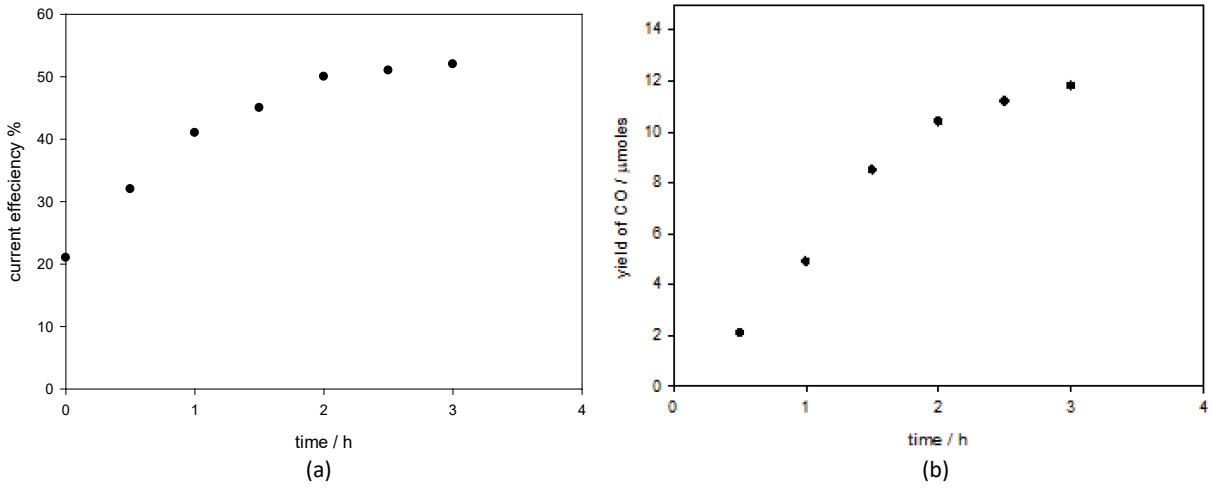

Figure 5. Variation of (a) current efficiency, and (b) CO yield with electrolysis time. Conditions: 0.5 mM Mn(TPP)Cl in presence of 0.6 M CF_3CH_2OH and saturated CO_2 (*ca* 0.23 M) 0.1M $[NBu_4][BF_4]$- MeCN.

It is important to note that the current efficiency and the amount of CO (in moles) increase over two hours and then become stable (Figure **5**). The current efficiency over three hours was ~ 52 % (~ 11.8 µmol of CO) while the turn-over number per hour decrease with electrolysis time, started ~ 1.6 then over three hours was 1.5 TN/h, which show the degradation of the Mn(TPP)Cl catalyst. However, the increasing of Mn(TPP)Cl concentration led to increase the CO yield and decrease H_2 yield.

Co-generation of CO and H_2 Upon Variation of Mn(TPP)Cl Catalysts Concentration

In separate experiments, the effect of different concentration of Mn(TPP)Cl on CO/H_2 production was also investigated (Figure 6 & Table 3). The time for each experiment was 3 h and the concentration of the catalyst was 0.05 mM, 0.1 mM, 0.2 mM, 0.35 mM and 0.5 mM. In general, higher the concentration of catalyst, the more CO and less H_2. This competitive reduction between H_2O and CO_2 was observed previously by Kubiak and co-worker.[39,40]

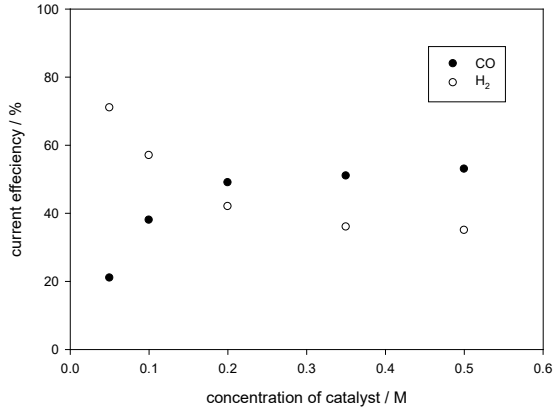

Figure 6. Co-generation CO and H_2 with different concentration of Mn(TPP)Cl. Conditions: 0.05 mM, 0.1 mM, 0.2 mM, 0.35 mM and 0.5 mM of Mn(TPP)Cl in presence of 0.6 M CF_3CH_2OH and saturated CO_2 (*ca* 0.23 M) 0.1 M $[NBu_4][BF_4]$-MeCN.

Table 3. Data for ECR of CO_2 by (0.5 mM, 2.5 µmol) Mn(TPP)Cl at carbon electrode.

Concentration of Mn(TPP)Cl / mM	0.05	0.1	0.2	0.35	0.5	0.05
n(CO) / µmol	3.1	6.5	9.3	11.1	12.7	3.1
n(H_2) / µmol	10.45	9.7	8.1	7.8	7.8	10.45
Current efficiency to produce CO (in %)	21	38	49	51	53	21
Current efficiency to produce H_2 (in %)	72	57	42	36	33	72
Charge passed, C	2.8	3.3	3.7	4.2	4.6	2.8

Mechanism of Carbon Dioxide Reduction and Formation of Products

Based on the earlier studies on Mn-complexes,[15,28,31,41] attempts have been made to delineate the mechanism by which Mn(TPP)Cl produced CO, H_2 and other products (Fig. 8). In a typical mechanism, metal center of the complex undergoes one or two electron reduction and react with CO_2 molecule. From the electrochemical data obtained (Fig. 1), it is evident that Mn(TPP)Cl undergoes a two-electron reduction processes leading to the formation of Mn(III)/Mn(II) and Mn(II)/Mn(I). Fig. 2 confirms that Mn(I) species is electro-catalytically active as CO_2 interacts near -1.3 V. Under this reduction potential window, Mn(I) species (**1**) coordinates with CO_2 to form metallacarboxylate species **2**. In the presence of high concentration of protons, there is a high probability of the formation of meta-stable metal-hydride intermediate, leading to the proton reduction and H_2 production. This step competes with the reduction of CO_2.[19,39] Therefore, **2** undergoes protonation to produce either metal hydride **2a** or carboxylated species **3**, which are responsible for different products found experimentally. For example, metal hydride **2a** undergoes decarboxylation to yield **2b** and then dehydrogenation to yield **1** along with 30–35 % H_2. On the other hand, carboxylated species **3** produce intermediate **4** through dehydration. The fact that the two-electron/two-proton reduction of CO_2 could also produce formate ($HCOO^-$),[42] we speculate that some of the species **3** degraded to produce side bicarbonate/formic acid (10–15 %). Finally, intermediate **4** undergoes decarbonylation to produce CO

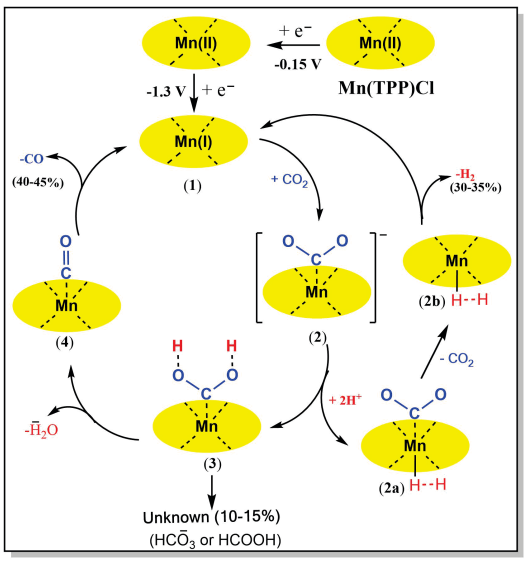

Figure 7. Possible mechanism of CO_2 reduction. Reduction condition: 0.5mM Mn(TPP)Cl in 0.1M $[Bu_4N][BF_4]$-MeCN. Scan rate 100 mV s^{-1}, vitreous carbon electrode under Ar at 25 °C.

(45–50 %) and active species **1**. It is worth highlighting that this mechanism also explains why Mn(TPP)Cl shows low catalytic performance as compared to other well-established Mn(I) complexes.[41] Generally, in high yielding Mn(I) catalyzed CO_2 ECR, the active species which interacts with electrophilic CO_2 is anionic intermediate (a nucleophile). However, in this case, the active species **1** is rather in +1 oxidation states, leading to weak interaction with the CO_2.

CONCLUSION

In this study, a Mn(III) complex Mn(TPP)Cl was employed as electrocatalyst for the ECR CO_2. The results of the study prove that complex Mn(TPP)Cl can efficiently reduce $CO_2 \rightarrow CO$ at a vitreous carbon electrode in $[Bu_4N][BF_4]$-MeCN electrolyte with reasonable current efficiency (~ 50- 55%). The reduction process and selectivity of the products significantly affected by the presence/absence of Brönsted acid (CF_3CH_2OH), the catalyst loading and electrolysis time. Unfortunately, TON (1.5 TN/h) and k_{cat} (0.12×10^2 M^{-1} s^{-1}) values were found to be slightly low.

Acknowledgment. Author is thankful to Dr. A. Haque, University of Hail, Saudi Arabia for his suggestion and proofreading during manuscript preparation.

REFERENCES

[1] G. A. Olah, G. S. Prakash, A. Goeppert, *J. Am. Chem. Soc.* **2011**, *133*, 12881–12898. https://doi.org/10.1021/ja202642y

[2] M. Mikkelsen, M. Jørgensen, F. C. Krebs, *Energy Environ. Sci.* **2010**, *3*, 43–81. https://doi.org/10.1039/B912904A

[3] C. Costentin, M. Robert, J.-M. Savéant, *Chem. Soc. Rev*. **2013**, *42*, 2423–2436. https://doi.org/10.1039/C2CS35360A

[4] C.-F. Leung, P.-Y. Ho, *Catalysts* **2019**, *9*, 760–786. https://doi.org/10.3390/catal9090760

[5] H. Schwarz, R. Dodson, *J. Phys. Chem*. **1989**, *93*, 409–414. https://doi.org/10.1021/j100338a079

[6] Y. Yamazaki, H. Takeda, O. Ishitani, *J. Photochem. Photobiol. C: Photochem. Rev*. **2015**, *25*, 106–137. https://doi.org/10.1016/j.jphotochemrev.2015.09.001

[7] T. Sakakura, J.-C. Choi, H. Yasuda, *Chem. Rev*. **2007**, *107,* 2365–2387. https://doi.org/10.1021/cr068357u

[8] D. L. DuBois, *Inorg. Chem*. **2014**, *53*, 3935–3960. https://doi.org/10.1021/ic4026969

[9] J. Schneider, H. Jia, J. T. Muckerman, E. Fujita, *Chem. Soc. Rev.* **2012**, *41*, 2036–2051. https://doi.org/10.1039/C1CS15278E

[10] J.-M. Savéant, *Chem. Rev.* **2008**, *108*, 2348–2378. https://doi.org/10.1021/cr068079z

[11] Y. Kuramochi, O. Ishitani, H. Ishida, *Coord. Chem. Rev*. **2018**, *373*, 333–356. https://doi.org/10.1016/j.ccr.2017.11.023

[12] C. D. Windle, R. N. Perutz, *Coord. Chem. Rev*. **2012**, *256*, 2562–2570. https://doi.org/10.1016/j.ccr.2012.03.010

[13] T. Yui, Y. Tamaki, K. Sekizawa, O. Ishitani, *Photocatalysis* **2011**, *303,* 151–184. https://doi.org/10.1007/128_2011_139

[14] H. Takeda, O. Ishitani, *Coord. Chem. Rev*. **2010**, *254*, 346–354. https://doi.org/10.1016/j.ccr.2009.09.030

[15] N. Corbin, J. Zeng, K. Williams, K. Manthiram, *Nano Research* **2019**, *12,* 1–33. https://doi.org/10.1007/s12274-019-2403-y

[16] A. J. Göttle, M. T. Koper, *J. Am. Chem. Soc*. **2018**, *140*, 4826–4834. https://doi.org/10.1021/jacs.7b11267

[17] C. Costentin, M. Robert, J.-M. Savéant, *Acc. Chem. Res.* **2015**, *48*, 2996–3006. https://doi.org/10.1021/acs.accounts.5b00262

[18] J. Bonin, A. Maurin, M. Robert, *Recent advances. Coord. Chem. Rev.* **2017**, *334*, 184–198. https://doi.org/10.1016/j.ccr.2016.09.005

[19] R. Francke, B. Schille, M. Roemelt, *Chem. Rev*. **2018**, *118*, 4631–4701. https://doi.org/10.1021/acs.chemrev.7b00459

[20] S. Fukuzumi, Y.-M. Lee, H.-S. Ahn, W. Nam, *Chem. Sci.* **2018**, *9*, 6017–6034. https://doi.org/10.1039/C8SC02220H

[21] C. Costentin, M. Robert, J.-M. Savéant, A. Tatin, *Proc. Natl. Acad. Sci. U.S.A.* **2015**, *112*, 6882–6886. https://doi.org/10.1073/pnas.1507063112

[22] Y. Zhang, J. Chen, P. E. Siegbahn, R.-Z. Liao, *ACS Catalysis* **2020**, in press.

[23] M. Bourrez, F. Molton, S. Chardon-Noblat, A. Deronzier, *Angew. Chem. Int. Ed.* **2011**, *50*, 9903–9906. https://doi.org/10.1002/anie.201103616

[24] B. Reuillard, K. H. Ly, T. E. Rosser, M. F. Kuehnel, I. Zebger, E. Reisner, *J. Am. Chem. Soc.* **2017**, *139*, 14425–14435. https://doi.org/10.1021/jacs.7b06269

[25] X. M. Hu, M. H. Rønne, S. U. Pedersen, T. Skrydstrup, K. Daasbjerg, *Angew. Chem. Int. Ed*. **2017**, *56*, 6468–6472. https://doi.org/10.1002/anie.201701104

[26] X. Zhang, Z. Wu, X. Zhang, L. Li, Y. Li, H. Xu, X. Li, X.;Yu, Z. Zhang, Y. Liang, *Nat. Comm.* **2017**, *8*, 14675. https://doi.org/10.1038/ncomms14675

[27] H. Takeda, C. Cometto, O. Ishitani, M. Robert, *ACS Catalysis* **2016**, *7*, 70–88. https://doi.org/10.1021/acscatal.6b02181

[28] B. Zhang, J. Zhang, J. Shi, D. Tan, L. Liu, F. Zhang, C. Lu, Z. Su, X. Tan, X.; Cheng, *Nat. Comm.* **2019**, *10*, 1–8. https://doi.org/10.1038/s41467-019-10854-1

[29] J.-X. Zhang, C.-Y. Hu, W. Wang, H. Wang, Z.-Y. Bian, *Appl. Catalysis A: General* **2016**, *522*, 145–151. https://doi.org/10.1016/j.apcata.2016.04.035

[30] K. Alenezi, K. Electrochemical Transformation of Alkanes, "Carbon Dioxide and Protons at Iron-Porphyrins and Iron-Sulfur Clusters", University of East Anglia, United Kingdom, **2013**.

[31] A. N. Marianov, Y. Jiang, *ACS Sustain. Chem. Eng*. **2019**, *7*, 3838–3848. https://doi.org/10.1021/acssuschemeng.8b04735

[32] K. Alenezi, *J. New Mater. Electrochem. Syst*. **2017**, *20*, 1–47. https://doi.org/10.14447/jnmes.v20i1.294

[33] K. Alenezi, *Int. J. Electrochem. Sci.* **2015**, *10*, 4279–4289.

[34] K. Alenezi, *Int. J. Electrochem. Sci* **2017**, *12*, 812–818. https://doi.org/10.20964/2017.01.58

[35] M. Hammouche, D. Lexa, M. Momenteau, J.-M. Saveant, *J. Am. Chem. Soc*. **1991**, *113*, 8455–8466. https://doi.org/10.1021/ja00022a038

[36] I. Bhugun, D. Lexa, J.-M. Savéant, *J. Am. Chem. Soc.* **1996**, *118*, 1769–1776. https://doi.org/10.1021/ja9534462

[37] M. Rakowski Dubois, D. L. Dubois, *Acc. Chem. Res.* **2009**, *42*, 1974–1982. https://doi.org/10.1021/ar900110c

[38] X. Lu, D. Y. Leung, H. Wang, M. K. Leung, M. K.; Xuan, *ChemElectroChem* **2014**, *1*, 836–849. https://doi.org/10.1002/celc.201300206

[39] E. E. Benson, C. P. Kubiak, A. J. Sathrum, J. M. Smieja, *Chem. Soc. Rev*. **2009**, *38*, 89–99. https://doi.org/10.1039/B804323J

[40] B. Kumar, J. M. Smieja, C. P. Kubiak*, J. Phys. Chem. C* **2010**, *114*, 14220–14223. https://doi.org/10.1021/jp105171b

[41] C. Steinlechner, A. F. Roesel, E. Oberem, A. Päpcke, N. Rockstroh, F. Gloaguen, S. Lochbrunner, R. Ludwig, A. Spannenberg, H. Junge, *ACS Catalysis* **2019**, *9*, 2091–2100. https://doi.org/10.1021/acscatal.8b03548

[42] N. D. Loewen, T. V. Neelakantan, L. A. Berben, *Acc. Chem. Res*. **2017**, *50*, 2362–2370. https://doi.org/10.1021/acs.accounts.7b00302